



# Determination of Chemical Exchange Rate in Chemical Exchange Saturation Transfer (CEST) Phenomenon in Magnetic Resonance Imaging through Analytical Solution of Bloch-McConnell Equations

M. R. Rezaeian<sup>1,\*</sup>

<sup>1</sup> Assistant Professor, Department of Biomedical Engineering, Hamedan University of Technology, Hamedan, Iran

ARTICLE INFO	ABSTRACT
<p>Article History:            Received 3 July 2021            Received in revised form 28 August 2021            Accepted 12 December 2021            Available online 13 December 2021</p>	<p>Magnetic Resonance Imaging (MRI), by enabling the non-invasive measurement of certain physiological markers, facilitates the study and tracking of molecular states, ultimately leading to the early diagnosis of diseases. Chemical Exchange Saturation Transfer (CEST) serves as a novel contrast mechanism in MRI for molecular studies. This contrast depends on multiple parameters, including relaxation times, the chemical exchange rate between water molecules and the contrast agent, the concentration of the contrast agent, and the properties of the applied radiofrequency (RF) pulse. The chemical exchange rate is a crucial parameter, as it correlates with various clinical indicators such as pH, temperature, and metabolite concentration. However, its direct measurement remains challenging. In this study, a method for determining this rate using RF pulse width is proposed. First, the CEST effect is expressed in an analytical relationship, demonstrating that this contrast reaches its maximum at a specific RF pulse width. This analytical expression distinguishes the CEST effect from the magnetic transfer effects caused by macromolecules in biological tissues, which act as confounding factors. Assuming a known contrast concentration, the chemical exchange rate can be determined through an analytical relationship based on the RF pulse width that maximizes the CEST effect. The validity of this analytical relationship is confirmed by comparison with widely accepted definitions of the CEST effect. Furthermore, by applying a Taylor series expansion to the analytical expression, relevant formulas from reputable publications are derived. The study employs validated data from a three-pool structure, which is consistent with biological tissue models referenced in authoritative sources. It is recommended that the findings of this study be practically implemented on MRI scanners.</p>
<p>Keywords:            Bloch-McConnell equations,            Chemical Exchange Saturation Transfer (CEST), Chemical Exchange Rate, Magnetization Transfer, Electromagnetic Pulse, Z-Spectrum.</p>	

## 1. INTRODUCTION

Saturation transfer experiments and studies, which have long been established for investigating small molecules and proteins, have led to the development of methods for tissue analysis and, subsequently, human body imaging. The processes involved in saturation transfer and their effects on living tissues are complex. Most of these methods

\* Corresponding Author: [mrezaeian@ut.ac.ir](mailto:mrezaeian@ut.ac.ir), [rezaeian2010@gmail.com](mailto:rezaeian2010@gmail.com)  
 Assistant Professor, Department of Biomedical Engineering, Hamedan University of Technology, Hamedan, Iran



rely on chemical exchange, making it challenging to distinguish between them due to their similar nature [1]. In the human body, saturation transfer is observed in macromolecules and semi-solid structures (Magnetization Transfer, MT), but its measurement using magnetic resonance techniques is difficult due to short transverse relaxation times ( $T_2$ ). However, in mobile structures, protein chains, and small peptides with longer  $T_2$  relaxation times—characteristic of slow chemical exchange mechanisms (CEST)—measurement becomes feasible. The MT effect, caused by semi-solid macromolecules, acts as an interfering factor in the assessment of CEST effects [1,2]. This effect has a resonance bandwidth of several kilohertz. MT was among the first imaging techniques based on saturation transfer, and it quickly gained clinical applications. This technique, which detects semi-solid and slow-relaxing components such as macromolecules, results in a broad Z-spectrum [3].

CEST contrast agents generally contain amide, amine, or hydroxyl groups. Based on tissue-specific properties and parameters such as exchange rates and chemical shift values, valuable information regarding the concentration and functionality of metabolic processes can be obtained. Exchange processes are essentially chemical reactions dependent on the molecular structure. The exchange rate for amide protons is in the range of  $s^{-1}$ , whereas for hydroxyl protons, it is approximately  $10,000 s^{-1}$ , and it varies with temperature, pH, and buffer properties of the solution. It can be asserted that this contrast is primarily defined by the exchange rate and the concentration of contrast agent protons. Consequently, Magnetic Resonance Spectroscopy (MRS) can be utilized to non-invasively study physiological parameters (such as intracellular pH, temperature, oxygen and energy consumption, and glucose metabolism) in living tissues [1,3,4].

By facilitating chemical exchange between the water pool and the contrast agent pool, indirect measurement of contrast agent protons can be achieved by observing changes in the water pool. During RF pulse application, saturation transferred to the water pool accumulates, leading to significant and measurable changes in the water proton signal. By enhancing this signal, indirect imaging of the contrast agent (which exists at a much lower concentration than body water hydrogen) can be performed through the water pool signal [1,3–6].

For chemical exchange to occur, selective labeling of a specific set of hydrogen atoms with an RF pulse at the Larmor frequency is required. As shown in Figure 1, the imaging pulse sequence used includes a rectangular saturation pulse with width  $t_{sat}$ , amplitude  $B_1$ , and frequency  $\omega$  (such RF pulses are commonly used), followed by an excitation pulse, spatial encoding, and image acquisition phase [7,8].

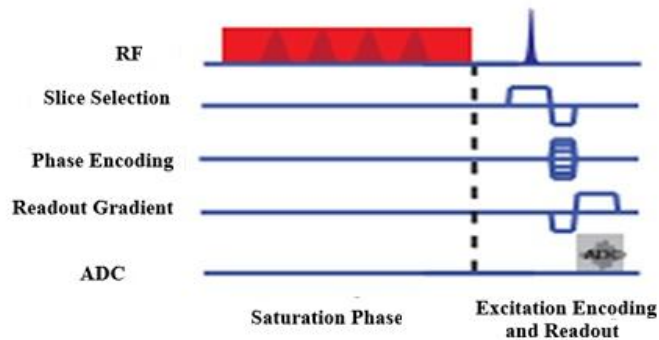


Fig. 1. Imaging Pulse Sequence in a CEST Imaging Experiment [7]

One of the most crucial approaches for deriving an analytical mathematical relationship describing CEST is based on the Z-spectrum. The Z-spectrum, which represents the normalized magnetization component along the Z-axis, is quantitatively described and analyzed using the Bloch-McConnell equations [7]. Due to the very low concentration of contrast agents compared to the hydrogen atoms in body water, this contrast effect results in a very small impact on the Z-spectrum. If the resonance frequency of the contrast agent is very close to that of water, its separation and detection become challenging. This issue becomes even more complex in real-world conditions when imaging the human body, where magnetization effects from other macromolecules also contribute to the signal.

Figure 2 illustrates the Z-spectrum obtained from mouse brain tissue. The most significant and strongest signal peak appears at 0 ppm (the water peak) and is caused by the direct saturation of water protons. The dependence of the Z-spectrum on the RF pulse amplitude and duration is also evident [7].

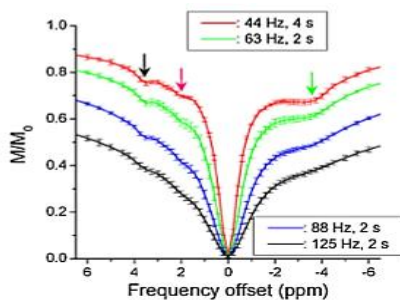


Fig. 2. Z-Spectrum Derived from Live Mouse Tissue at Different RF Pulse Amplitudes and Durations [7]

For diamagnetic CEST agents with low exchange rates, increasing the RF pulse duration enhances the CEST effect. Thus, transient response extraction is not critical in such cases. However, for PARACEST agents with high exchange rates, prolonging the pulse duration does not necessarily maximize the CEST effect. Therefore, determining the optimal pulse width that maximizes the CEST effect requires transient response analysis, as reported by Jin et al. [7,9].

Several methods for measuring exchange rates have been reported [7,10]. Sun proposed a method for diamagnetic agents based on an empirical definition that simultaneously estimates the exchange rate and contrast agent concentration using the optimal RF pulse amplitude, without considering MT effects [10]. Currently, paramagnetic agents are of particular interest due to their high Larmor frequencies, which allow them to be well separated from the water resonance frequency. This separation reduces the direct saturation effect and facilitates direct measurement of the CEST effect itself [1,3-5].

In any in vivo saturation transfer experiment, macromolecular effects commonly referred to as the MT effect are inevitable [2]. Accordingly, two primary confounding factors in CEST measurement are direct saturation and MT effects. Numerous studies have been conducted to isolate the pure CEST effect from these interfering factors [1,3-5,7]. One of the most widely used and experimentally validated methods is  $MTR_{asym}$ , frequently cited in the literature. In this approach, the Z-spectrum is measured twice: once by increasing and once by decreasing the resonance frequency. The difference between these two Z-spectra reflects the CEST effect, as the CEST signal is inherently asymmetric and occurs only at positive frequencies, unlike direct saturation and MT effects, which are symmetric [1,3-5,7].

This study focuses on paramagnetic agents while accounting for MT effects, proposing an RF pulse duration-based approach for exchange rate estimation. Since  $MTR_{asym}$  alone does not allow for the derivation of an analytical pulse width relationship in paramagnetic CEST experiments, an alternative definition, closely aligned with  $MTR_{asym}$  but free from confounding factors, is adopted to enable analytical pulse width computation [11].

The structure of the paper is as follows: First, a mathematical formulation of the CEST effect under the defined conditions is presented for transient response analysis in a three-pool system (water, CEST, and MT) [11]. Then, the optimal RF pulse duration is determined by differentiating the transient response function, establishing a relationship between the optimal pulse width and the chemical exchange rate. Finally, simulation data are introduced, followed by a discussion of results and recommendations.

## 2. TRANSIENT RESPONSE OF THE Z-SPECTRUM

The Bloch-McConnell equations serve as a suitable analytical tool for modeling and describing the Z-spectrum. These equations, derived from the Bloch equations, can be applied in environments with different chemical

properties. The simplest case involves a two-pool model, while more complex scenarios require multi-pool models for representation and generalization.

During the application of an off-resonance RF pulse, under certain conditions, the only influential factor affecting the longitudinal magnetization component  $Z$  of the water pool can be expressed by the following equation as a decaying exponential function with a time constant  $R_{1\rho}(\omega)$  [7,12].

$$Z(\omega, t) = (P_{zeff}P_z.Z_i - Z^{ss}(\omega)).e^{-R_{1\rho}(\omega).t} + Z^{ss}(\omega) \quad (1)$$

In this equation,  $Z_i$  and  $Z^{ss}$  represent the initial value of the normalized longitudinal magnetization and the steady-state response (final value), respectively.

$$Z_i = |M_i|/M_0, \quad Z^{ss}(\omega) = P_z \frac{R_{1res}}{R_{1\rho}(\omega)} \quad (2)$$

$P_{zeff}$  and  $P_z$  are projection coefficients, both of which are considered equal to  $\cos \theta$  for CEST experiments (where  $\theta$  follows its previous definition and represents the angle between the magnetization vector  $M$  and the axis). Essentially, these coefficients describe the resultant magnetization vector in the rotating frame of reference. The term  $R_{1res}$  is approximately calculated using the relation  $R_{1res} \approx \cos \theta \cdot R_{1a}$ . Theoretical calculations by Zaiss et al. derived  $R_{1\rho}(\omega)$  in a three-pool model, incorporating the MT effect, using the following equation [13].

$$R_{1\rho mt}(\omega) = R_{eff}(\omega) + \frac{R_{ex,b}(\omega)}{1+f_c} + R_{ex,c}(\omega) \quad (3)$$

Here,  $R_{eff}$  represents the relaxation rate of water protons in the rotating frame, while  $R_{ex}$  denotes the exchange-induced relaxation rate in the rotating frame for different pools bbb and ccc. The pools b and c correspond to the contrast agent (CEST effect) and macromolecules (MT effect), respectively [7]. Zaiss also argued that under the influence of the MT pool, the longitudinal relaxation time of the water pool is altered, and this effect has been incorporated into the formulation [13].

$$R_{1amt} = \frac{1}{2}(k_{ac} + k_{ca} + R_{1a} + R_{1c} - \sqrt{(k_{ac} + k_{ca} + R_{1a} + R_{1c})^2 - 4(k_{ca}R_{1a} + k_{ac}R_{1c} + R_{1a}R_{1c})}) \approx \frac{R_{1a}+f_cR_{1c}}{1+f_c} \quad (4)$$

In other words,  $R_{1amt}$  and  $R_{1\rho mt}$  replace  $R_{1a}$  and  $R_{1\rho}$ , respectively. If the concentration  $f_c$  decreases (or more precisely, as  $f_c \rightarrow 0$ ), then  $R_{1amt} \cdot R_{1\rho mt}$ ,  $R_{1a} \cdot R_{1\rho}$  will be exactly equal.

### 3. ANALYTICAL EXTRACTION OF CEST EFFECT

To obtain a definition of the CEST effect that effectively eliminates the direct water saturation and MT effects, the  $Z$ -spectrum is calculated once in the absence of the CEST agent and again in its presence [11].

$$MTR(\omega, t_{sat}) = Z(\omega, t_{sat})|_{R_{ex}=0} - Z(\omega, t_{sat}) \quad (5)$$

By substituting the above relations, an analytical equation for three-pool systems is derived. That is:

$$R_{1\rho}(\omega)|_{3-pool} = R_{eff}(\omega) + \frac{R_{ex}^b(\omega)}{1+f_c} + R_{ex}^c(\omega) \quad (6)$$

and

$$R_{1\rho}(\omega)|_{3-pool}, R_{ex}^b = 0 = R_{eff}(\omega) + R_{ex}^c(\omega) \quad (7)$$

By substituting relations (6) and (7) into equation (5) and considering relation (1), equation (8) is obtained.

$$MTR(\omega, t_{sat})|_{3-pool} = \cos^2 \theta.$$

$$\left\{ \left[ \left( 1 - \frac{R_{1amt}}{R_{eff}(\omega) + R_{ex}^c(\omega)} \right) \cdot e^{-(R_{eff}(\omega) + R_{ex}^c(\omega))t_{sat}} + \frac{R_{1amt}}{R_{eff}(\omega) + R_{ex}^c(\omega)} \right] - \left[ \left( 1 - \frac{R_{1amt}}{R_{eff}(\omega) + \frac{R_{ex}^b(\omega)}{1+f_c} + R_{ex}^c(\omega)} \right) \cdot e^{-(R_{eff}(\omega) + \frac{R_{ex}^b(\omega)}{1+f_c} + R_{ex}^c(\omega))t_{sat}} + \frac{R_{1amt}}{R_{eff}(\omega) + \frac{R_{ex}^b(\omega)}{1+f_c} + R_{ex}^c(\omega)} \right] \right\} \quad (8)$$

#### 4. EXTRACTION OF OPTIMAL PULSE DURATION

The optimal pulse duration is determined through relation (8) as an appropriate objective function for describing the CEST effect. By differentiating relation (8) with respect to the pulse duration and simplifying, the optimal pulse duration in three-pool systems is obtained from the closed-form equation (9).

$$t_{sat,opt}(\omega) | 3 - pool = \frac{1}{R_{ex}^b(\omega)} \cdot \log \left( \frac{\left( 1 - \frac{R_{1amt}}{R_{eff}(\omega) + \frac{R_{ex}^b(\omega)}{1+f_c} + R_{ex}^c(\omega)} \right) \cdot (R_{eff}(\omega) + \frac{R_{ex}^b(\omega)}{1+f_c} + R_{ex}^c(\omega))}{\left( 1 - \frac{R_{1amt}}{R_{eff}(\omega) + R_{ex}^c(\omega)} \right) \cdot (R_{eff}(\omega) + R_{ex}^c(\omega))} \right) \quad (9)$$

By considering relation (9) at the resonance frequency of pool b, which corresponds to the CEST agent, relation (10) is obtained.

$$t_{sat,opt}(\omega_b) | 3 - pool = \frac{1}{R_{ex}^b(\omega_b)} \cdot \log \left( \frac{P_{zeff} \cdot (R_{eff}(\omega_b) + \frac{R_{ex}^b(\omega_b)}{1+f_c} + R_{ex}^c(\omega_b)) - R_{1amt} \cdot \cos \theta}{P_{zeff} \cdot (R_{eff}(\omega_b) + R_{ex}^c(\omega_b)) - R_{1amt} \cdot \cos \theta} \right) \quad (10)$$

#### 5. DATABASE

A valid dataset has been used to evaluate the system and ensure the accuracy of the results. A sufficiently large number of data points is required. This data was reported by Guerke and colleagues based on a creatine phantom in a 4.9 Tesla field. The values of these parameters are consistent with the muscle values of the body in the field, as shown in Table 1 [14].

**Table 1.** Simulation parameter values in a three-pool system in a 4.9 Tesla field, according to the report by Guerke et al. [14].

Parameters	$\delta\omega(ppm)$	$k(s^{-1})$	$f$	$T_2$ (s)	$T_1$ (s)
Simulation data					
Water pool (a)				0/050	1/412
CEST agent pool (b)	1/9	1500	0/0014	0/015	1/412
MT effect pool (c)	0	66	0/074	/0000087	1

#### 6. RESULTS

This section is divided into several sub-sections. The first part compares the validity of the relation used to define the CEST effect with the widely accepted and referenced definition, which is consistent with the results derived from experimental studies ( $MTR_{asym}$ ). This comparison is made across different RF pulse ranges and varying chemical exchange rates. Next, the dependence of the RF pulse width on the CEST effect is examined. It is shown that there exists an optimal RF pulse width at which the CEST effect reaches its maximum value. Finally, the relationship between RF pulse width and the chemical exchange rate is demonstrated, supporting the feasibility of measuring the chemical exchange rate based on the RF pulse width, provided the contrast agent concentration is known.

##### 6.1. Validation of the CEST Effect Definition

$MTR_{asym}$  is a widely recognized, reliable, and referenced metric in many scientific and experimental studies. Since all claims in this paper are based on a definition that differs from  $MTR_{asym}$ , a need for a distinct definition was previously stated specifically, the necessity for an analytical relation that accounts for destructive effects (direct water saturation and MT effect). Therefore, the accuracy of this definition is initially examined under various conditions. Minor differences and similar behaviors across conditions could serve as evidence supporting the validity of this approach. It should be noted that other studies have also simultaneously determined the optimal pulse width and amplitude using this definition. In this section, using the dataset provided in Table 1, both  $MTR_{asym}$  and the CEST effect derived from relation (8) are calculated and compared across various values. Figure 3 compares the spectral similarity of the two metrics across different RF pulse amplitudes (3, 5, 7, and 9 microtesla) and chemical exchange rates (700, 1000, 1300, and 1600  $s^{-1}$ ). The resonance frequency range is varied from 0 to 5 ppm.

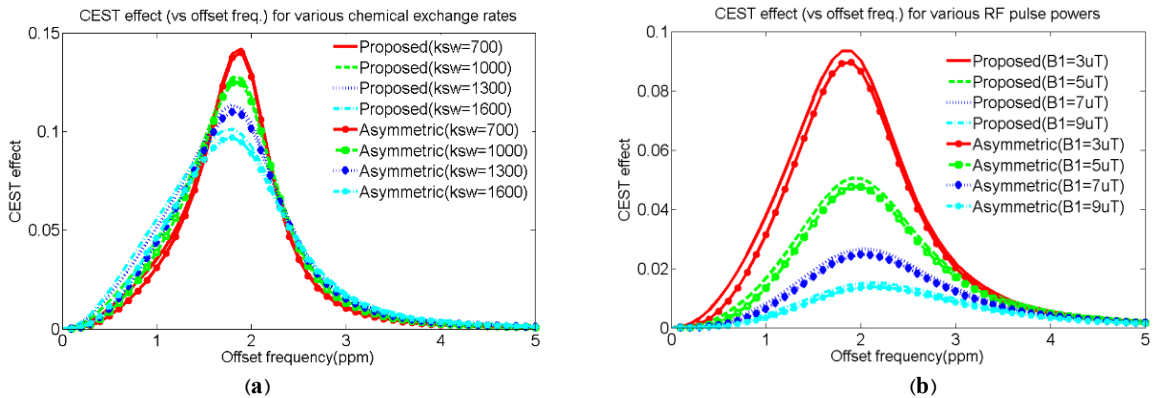


**Fig. 3.** Changes in the CEST effect spectrum according to the  $MTR_{asym}$  criterion and the definition derived from relation (8) in (a) different amplitudes and (b) varying exchange rates.

### 6.2. Dependence of the CEST Effect on RF Pulse Width

After confirming the validity of the definition used (relation (8)) of the CEST effect, as outlined in section 6-1, the dependence of the CEST effect on the RF pulse width is investigated. A key observation in this section is the existence of an optimal pulse width at which the CEST effect reaches its maximum. Given that the proposed definition is a well-defined and continuous function based on physical values in line with human physiology, it can be concluded that this function is differentiable (at least within the studied range). In Figure 4, variations in the RF pulse width in the range of 0.5, 1, 2, and 10 seconds and their effects on the CEST spectrum are shown. As observed in Figure 4, the CEST effect reaches its maximum value at a pulse width of 2 seconds.

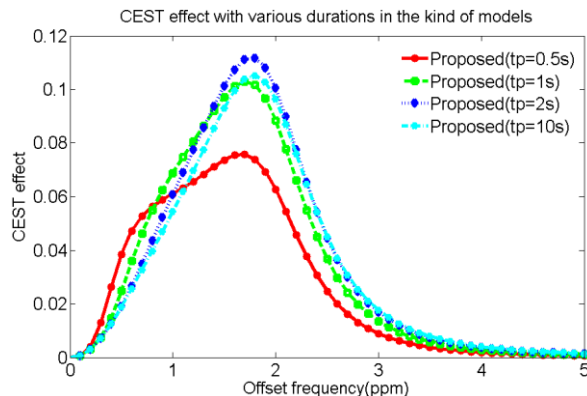


**Fig. 4.** Changes in the CEST effect spectrum based on relation (8) at different pulse widths.

### 6.3. Dependence of Chemical Exchange Rate on RF Pulse Width

In this section, instead of examining the entire CEST effect spectrum, only a frequency component at 1.9 ppm, corresponding to the resonance frequency of the contrast agent pool (Larmor frequency), is considered. In Figure 5-a, the changes in the CEST effect at resonance frequency are shown for different RF pulse widths as the chemical exchange rate varies (800, 1000, 1200, and 1600 per second). As observed at all exchange rates, with an increase in pulse width, the CEST effect increases. However, after a certain point, further increase in pulse width no longer contributes to the increase in the CEST effect, and it starts to decrease before eventually stabilizing. This implies that increasing the duration and width of the pulse will not further enhance the CEST effect.

In Figure 5-b, the optimal pulse width variations obtained from relation (10) are plotted against changes in the chemical exchange rate at the resonance frequency of 1.9 ppm. Interestingly, the changes shown are nearly linear.

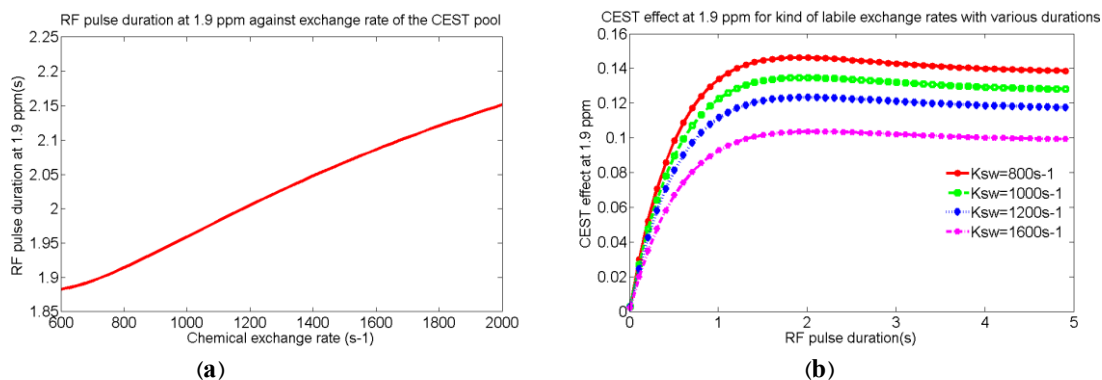


**Figure 5-a** - Changes in the CEST effect at Larmor frequency (1.9 ppm) with different RF pulse widths for exchange rates of 800, 1000, 1200, and 1600 per second. **Figure 5-b** - Changes in RF pulse width at Larmor frequency for different chemical exchange rates.

## 7. SUMMARY (DISCUSSION AND SUGGESTIONS)

This paper presents a solution for measuring chemical exchange rates, a critical factor in clinical and physiological studies. Various methods have been suggested for this purpose so far [7, 10]. In one of these methods, San successfully measured the exchange rate by assessing the RF pulse amplitude [10]. San showed that there is an RF pulse amplitude that can maximize the CEST effect. Essentially, San proposed a method where by measuring the optimal pulse amplitude and the maximum CEST effect at this optimal amplitude, the exchange rate could be determined. However, San's focus was on diamagnetic CEST agents, which have low to moderate exchange rates, and did not account for the MT effect from the body's macromolecules.

The focus of this study is on paramagnetic CEST agents, which have gained significant efficiency recently for several reasons. Additionally, to ensure the study aligns more with real-body conditions, the MT effect was mathematically modeled and analyzed. To achieve this, an accurate analytical definition of the CEST effect, considering the destructive MT and direct saturation effects, was initially required. This analytical definition serves as an objective function that is dependent on the RF pulse width. By deriving it with respect to time, an optimal pulse width that maximizes the CEST effect was presented in a closed-form mathematical formula. This function is well-defined, continuous, and differentiable at least within the study's working range because it pertains to physical values.

A noteworthy finding is the relatively linear dependence between the optimal RF pulse width and the chemical exchange rate. Thus, similar to San, this paper claims it can measure the chemical exchange rate, with the difference being that this study uses the RF pulse width rather than the pulse amplitude.

To evaluate the claim made in this paper, two approaches are followed. First, the validity of the optimal pulse width formula is checked by comparing it with results reported in other papers. Then, an attempt is made to compare the actual chemical exchange rate with the estimated exchange rate (based on this paper). This comparison is fitted into a quadratic equation, and a linear relationship is expected.

In the first evaluation step, by applying the Taylor series expansion of the logarithmic function in the pulse width formula (equation 10), an approximate relationship is obtained. This approximation closely resembles Jin's relation [9]. However, writing the Taylor expansion requires some considerations, particularly ensuring that the logarithmic argument involves only limited changes.

$$\text{Log}(x) = -(1 - x) - (1 - x)^2/2 - (1 - x)^3/3 - \dots \quad \text{for } 0 < x < 2 \tag{11}$$

Assuming the conditions for the Taylor series hold, equation (10) will be transformed into equation (12).

$$t_{p,opt}|_{2 - pool, approximat} = \left(\frac{1}{R_{exl}}\right) \cdot \left[ -\left(1 - \frac{R_{eff} + R_{ex} - R_{1a}}{R_{eff} - R_{1a}}\right) - \left(1 - \frac{R_{eff} + R_{ex} - R_{1a}}{R_{eff} - R_{1a}}\right)^2/2 - \left(1 - \frac{R_{eff} + R_{ex} - R_{1a}}{R_{eff} - R_{1a}}\right)^3/3 - \dots \right] \tag{12}$$

Assuming  $-1 < 1 - x < 1$ , it can be claimed that raising the terms of the Taylor series to higher powers will cause the remaining terms to become smaller. Therefore, by considering only the first term, the approximate response of equation (13) is obtained. It is worth mentioning that Jin had previously calculated the optimal pulse width in a two-pool system, so equation (10) is written and approximated for the two-pool system.

$$t_{p,opt}|_{2 - pool, approximat} \approx \frac{1}{R_{eff} - R_{1w}} \tag{13}$$

In the execution of the second step of the evaluation, similar to San in [10], an attempt is made to establish a relationship between the actual chemical exchange rate and the measured one based on this paper, using the least squares (MSE) algorithm, and it is then fitted.

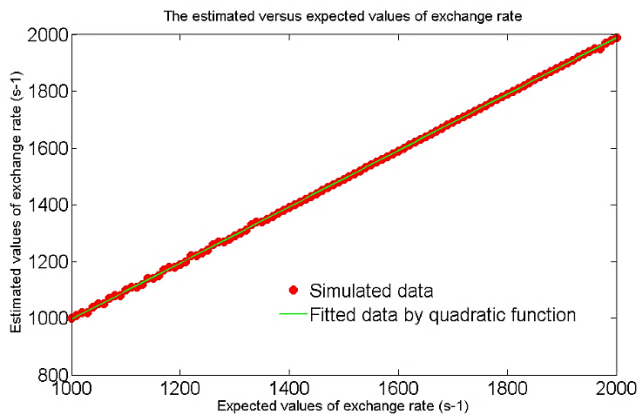


Fig. 6. Evaluation of the measured chemical exchange rate based on equation (10) as a function of RF pulse width. The estimated and actual chemical exchange rates are compared in the range of 1000 to 2000 seconds.

The fitting results of the obtained samples, based on the least squares algorithm, shown in Figure 6, indicate a strong proximity to a straight line. Note that the value of 5 widths from the origin within the range of 1000 to 2000 is very negligible. The slope of the line is also very close to one with high precision.

$$k_{sw}|_{estimated} = - 2.5422 \times 10^{-6} k_{sw,expected}^2 + 0.9996 k_{sw,expected} - 5.1192$$

This section presents suggestions for continuing and enhancing this research. In this study, it was assumed that the concentration of the contrast agent is known and fixed. It is suggested that a solution be provided to simultaneously determine both the exchange rate and the concentration. Furthermore, all stages of this research were based on simulation data, so it is recommended that, with the provision of suitable conditions for implementing CEST imaging protocols on MRI scanners, the practical implementation of this algorithm be made possible.

### **Transparency Statement**

The data supporting this study are available upon reasonable request to the corresponding author, subject to ethical and confidentiality considerations.

### **Acknowledgments**

We would like to express our gratitude to all individuals who contributed to this project.

### **Declaration of Interest**

The authors declare that they have no competing interests.

### **Funding**

This research received no specific grant from any funding agency, commercial, or not-for-profit sectors.

### **REFERENCES**

- [1] Zijl, P. C. M. V., & Yadav, N. (2011). Chemical exchange saturation transfer (CEST): What is in a name and what isn't? *Magnetic Resonance in Medicine*, 65(4), 927-948. <https://doi.org/10.1002/mrm.22761>
- [2] Desmond, K. L., & Stanisiz, G. J. (2012). Understanding quantitative pulsed CEST in the presence of MT. *Magnetic Resonance in Medicine*, 67(4), 979-990. <https://doi.org/10.1002/mrm.23074>
- [3] Consolino, L., Irrera, P., Romdhane, F., Anemone, A., & Longo, D. (2021). Investigating plasma volume expanders as novel macromolecular MRI-CEST contrast agents for tumor contrast-enhanced imaging. *Magnetic Resonance in Medicine*, 86, 1007-995. <https://doi.org/10.1002/mrm.28778>
- [4] Vinogradov, E., Sherry, A. D., & Lenkinski, R. E. (2012). CEST: From basic principles to applications, challenges, and opportunities. *Journal of Magnetic Resonance*, 229, 155-172. <https://doi.org/10.1016/j.jmr.2012.11.024>
- [5] Liu, G., Song, X., Chan, K. W., & McMahon, M. T. (2013). Nuts and bolts of chemical exchange saturation transfer MRI. *NMR in Biomedicine*, 26(7), 810-828. <https://doi.org/10.1002/nbm.2899>
- [6] Woods, M., Woessner, D. E., & Sherry, A. D. (2006). Paramagnetic lanthanide complexes as PARACEST agents for medical imaging. *Chemical Society Reviews*, 35(6), 500-511. <https://doi.org/10.1039/b509907m>
- [7] Zaiss, M., & Bachert, P. (2013). Chemical exchange saturation transfer (CEST) and MR Z-spectroscopy in vivo: A review of theoretical approaches and methods. *Physics in Medicine and Biology*, 58(22), 221-269. <https://doi.org/10.1088/0031-9155/58/22/R221>
- [8] Ward, K. M., Aletras, A. H., & Balaban, R. S. (2000). A new class of CAs for MRI based on proton chemical exchange dependent saturating transfer (CEST). *Journal of Magnetic Resonance*, 143(55), 79-87. <https://doi.org/10.1006/jmre.1999.1956>
- [9] Jin, T., Wang, P., Zong, K., & Kim, S. (2012). Magnetic resonance imaging of the amine-proton exchange

(APEX) dependent contrast. NeuroImage, 59(2), 1218-1227.  
<https://doi.org/10.1016/j.neuroimage.2011.08.014>

- [10] Sun, P. Z. (2010). Simultaneous determination of labile proton concentration and exchange rate utilizing optimal RF power: Radio frequency power (RFP) dependence of chemical exchange saturation transfer (CEST) MRI. *Journal of Magnetic Resonance*, 202(2), 155-161. <https://doi.org/10.1016/j.jmr.2009.10.012>
- [11] Rezaeian, M. R., Hossien-Zadeh, G. A., & Soltanian-Zadeh, H. (2016). Simultaneously optimizing power and duration of RF pulse in the paracest MRI. *Magnetic Resonance Imaging*, 34(6), 743-753. <https://doi.org/10.1016/j.mri.2016.02.001>
- [12] Trott, O., & Palmer, A. G. (2004). Theoretical study of  $R(1\rho)$  rotating-frame and  $R_2$  free-precession relaxation in the presence of n-site chemical exchange. *Journal of Magnetic Resonance*, 170(1), 104-112. <https://doi.org/10.1016/j.jmr.2004.06.005>
- [13] Zaiss, M., Zu, Z., Xu, J., Schuenke, P., Gochberg, D. F., Gore, J. C., Ladd, M. E., & Bachert, P. (2015). A combined analytical solution for chemical exchange saturation transfer and semi-solid magnetization transfer. *NMR in Biomedicine*, 28(2), 217-230. <https://doi.org/10.1002/nbm.3237>
- [14] Goerke, S., Zaiss, M., & Bachert, P. (2014). Characterization of creatine guanidinium proton exchange by water-exchange (WEX) spectroscopy for absolute pH CEST imaging in vitro. *NMR in Biomedicine*, 27(5), 507-518. <https://doi.org/10.1002/nbm.3086>